Gas-Phase Reactions of O- and OH-Containing Cr Cluster Ions with Ethylene Molecules: Isolation of Reaction Sites of Cr-Containing Catalysts for Ethylene Polymerization

Tetsu Hanmura,[†] Masahiko Ichihashi,[‡] Takashi Monoi,[§,||] Kazuo Matsuura,[§,⊥] and Tamotsu Kondow*[,‡]

East Tokyo Laboratory, Genesis Research Institute, Inc., 717-86 Futamata, Ichikawa, Chiba 272-0001, Japan, Cluster Research Laboratory, Toyota Technological Institute, in East Tokyo Laboratory, Genesis Research Institute, Inc., 717-86 Futamata, Ichikawa, Chiba 272-0001, Japan, and Research & Development Center, Japan Polyolefins Co., Ltd., 10-1 Chidori-cho, Kawasaki-ku, Kawasaki, Kanagawa 210-8547, Japan

Received: March 31, 2004; In Final Form: August 26, 2004

Reactions of ethylene molecules on Cr_n^+ ($n = 1-4$), Cr_nO^+ ($n = 1-4$), and Cr_nOH^+ ($n = 1, 2$) were studied in a tandem mass spectrometer equipped with a reaction cell. The mass spectra of the product ions showed that (1) under a single collision condition, oxidation of ethylene and chromium pickup (Cr-pickup) by ethylene take place on Cr_n^+ ($n = 2-4$), Cr_nO^+ ($n = 2-4$), and Cr_nOH^+ ($n = 2$), and (2) under a multiple collision condition, two ethylene molecules are chemisorbed exclusively on CrO^+ and $CrOH^+$; the ethylene molecules seem to be dimerized in comparison with our preliminary density functional theory calculation. Size and collision-energy dependences of the reaction cross sections lead us to conclude that the Cr-pickup reaction proceeds via an intermediate in which C_2H_4 is chemisorbed on a parent ion. The preferential ethylene dimerization on CrO^+ and $CrOH^+$ implies that, on a silica-supported chromium catalyst (Philips catalyst), ethylene polymerization proceeds preferentially on active centers consisting of atomic chromium bonded to O or OH of the substrate.

1. Introduction

Metal clusters isolated in the gas phase exhibit specific size dependence in their reactivity.[1,2] This size-specific reactivity of the metal clusters should have practical importance in designing a catalyst which is composed of metal clusters dispersed on a substrate, because the reactivity of the metal clusters on the substrate is closely related to that of the isolated metal clusters. In addition, clusters with any size are easily prepared in the gas phase. Therefore, one could optimize the size and the geometry of the metal clusters for reactivity and selectivity and, taking advantage of this information, identify the most favorable metal cluster having a specific component and a geometry, which is regarded as an "active center".

In a practical catalytic reaction, the concept of the active center is successfully used to explain the reaction scheme,[3] but there is no direct way to prove the existence and to identify it. Let us consider the Phillips catalyst for ethylene polymerization, which is composed of chromium supported typically on a silica powder.[4−7] Many variants of the original catalyst have been developed on the basis of empirical knowledge, mainly because ethylene polymerization is of industrial importance. Intensive investigations have revealed that only several percent of chromium in the catalyst is involved in catalytic polymerization of ethylene,[8−10] while the rate of the ethylene polymerization and the properties of the resulting polyethylene change sensitively with changing the composition and the structure of its support, the procedure of the preparation of the catalyst, the activation method of the catalyst, and so forth.[11−13] These investigations indicate that the polymerization proceeds most efficiently on an active center made from chromium and its substrate. However, despite extensive studies for several decades, there are still controversial arguments on identification of the active center(s);[14] for instance, one insists that a monomeric chromium is the active center[5,15] while another reports that a dimeric chromium is the one.[16,17]

As described above, the active center could be identified by using a corresponding reaction in the gas phase by taking advantage of the fact that any metallic species postulated as the candidates of the active center(s) can easily be prepared in the gas phase. To elucidate the active center of the Phillips catalyst, we investigated the reaction of ethylene molecules on Cr_n^+ ($n = 1-4$), Cr_nO^+ ($n = 1-4$), and Cr_nOH^+ ($n = 1, 2$) at the lowest possible collision energy to minimize energy introduced by the collision. In this reaction, we chose chromium cluster ions and their monoxides and hydroxides because (1) ions are easily mass-selected, (2) chromium is the major metallic component of the Phillips catalyst, and (3) chromium is bonded to the substrate to form chromium monoxide and hydroxide, on the basis of the fact that reactions on metal clusters in which d-electrons play a central role are insensitive to the change of the charge state.[18,19]

2. Experimental Section

The apparatus employed in the present study is described briefly because its detail has been published elsewhere.[20,21] A schematic diagram of the apparatus is shown in Figure 1. The apparatus consists of a cluster ion source, a cooling cell, quadrupole mass filters, a reaction cell, and a detector, which

* Corresponding author. E-mail: kondow@clusterlab.jp.
[†] East Tokyo Laboratory, Genesis Research Institute, Inc.
[‡] Cluster Research Laboratory, Toyota Technological Institute.
[§] Research & Development Center, Japan Polyolefins Co., Ltd.
[||] Present affiliation: Japan Polyethylene Corp., Japan.
[⊥] Present affiliation: KM Techno Research, Japan.

10.1021/jp0402582 CCC: $27.50
Published on Web 10/30/2004

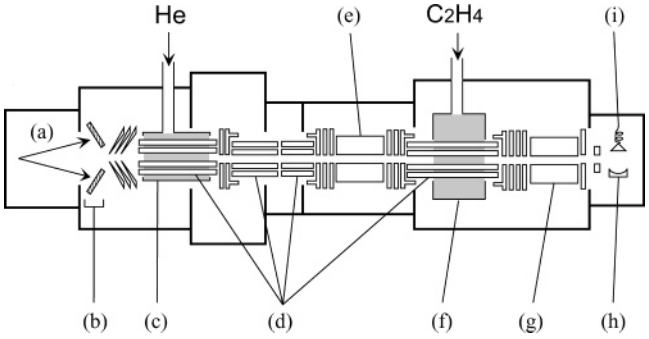

Figure 1. A schematic view of the apparatus: (a) xenon (or argon) ion beam, (b) chromium targets, (c) cooling cell, (d) octopole ion guides, (e) first quadrupole mass filter, (f) reaction cell, (g) second quadrupole mass filter, (h) ion conversion dynode, and (i) secondary electron multiplier.

are connected by octopole ion guides for efficient cluster ion transportation. Cluster ions were produced by sputtering a rare gas (xenon or argon) ion beam on four chromium targets at a collision energy up to 15 keV; the rare gas ion beam was prepared in a plasma ion source (CORDIS Ar25/35c, Rokion Ionenstahl-Technologie). In addition, monoxides and hydroxides of chromium cluster ions (Cr_nO^+ and Cr_nOH^+) emerged without introducing any oxygen gas, probably due to the reaction of Cr_n^+ mainly with residual impurities present in the vacuum chamber. The cluster ions were admitted in the cooling cell of 400 mm in length filled with helium gas (pressure of $>10^{-3}$ Torr) at a temperature of 300 K and were cooled by more than 100 collisions with He atoms, which are sufficient to cool the cluster ions down to 300 K on the basis of the fact that Al_2^+ and Al_{11}^+ have been proven to be thermalized by 50 and 100 collisions, respectively.[22] The cluster ions thus cooled were admitted into the first quadrupole mass filter for selection of cluster ions of a given size. The size-selected cluster ions were introduced into the second octopole ion guide surrounded by a reaction cell in which the incoming cluster ions react with ethylene molecules, C_2H_4, introduced through a variable leak valve (Granville-Phillips, Series 203). The ethylene gas (Takachiho Chemical, >99.9%) was used without further purification. The pressure in the reaction cell, which was measured by a spinning rotor gauge (MKS, SRG-2), was varied in the range of 3×10^{-5} to 9×10^{-4} Torr. The single collision condition is fulfilled at a pressure lower than 2×10^{-4} Torr because the product intensities were found to increase in proportion to the pressure up to this pressure, while multiple collision of ethylene was found to take place above this pressure because the product intensities deviate from the linear relationship at a pressure higher than this pressure. Product ions which came out of the reaction cell were mass-analyzed in the second quadrupole mass filter and were detected by an ion conversion dynode followed by a secondary electron multiplier (Murata Ceratron, EMS-6081B) in a pulse counting mode. Signals from the secondary electron multiplier were processed in an electronic circuitry based on a personal computer. The spread of the translational energy of the parent cluster ions was measured to be typically 3 eV in the laboratory frame by applying a retarding voltage to the octopole ion guide mounted in the reaction cell. This energy spread gives rise to the uncertainty of about ± 0.2 eV in the center-of-mass frame in a collision involving a Cr_3^+ ion, and larger for smaller cluster ions.

In practice, the first and the second mass filters are so tuned that the first one isolates a parent cluster ion of interest and the second one facilitates (1) the assignment of the product ions and (2) the determination of the reaction cross sections. The mass resolution of the first mass filter was set to be sufficiently high to isolate a parent cluster ion of interest from other undesired ions; for example, the mass resolution ($m/\Delta m$) of 150 is high enough to isolate $CrOH^+$ from CrO^+. The mass resolution of the second mass filter was set to be high enough to assign the product ions; a mass resolution of 100−400 was a typical value. In the measurement of the reaction cross sections, the mass resolution was sacrificed for gaining the peak intensity; the typical mass resolution was about 30. Figure 2a,b shows the mass spectra of CrO^+ and $CrOH^+$, respectively, measured by using the first and the second mass filters in a tandem arrangement with a mass resolution of ∼150 for both the mass filters. Note that the 69 amu peak (see panel b) consists of ∼95% of $^{52}CrOH^+$ and ∼5% of $^{53}CrO^+$. The correction was made in obtaining the cross sections for the reactions involving $CrOH^+$ as described in section 3.2.

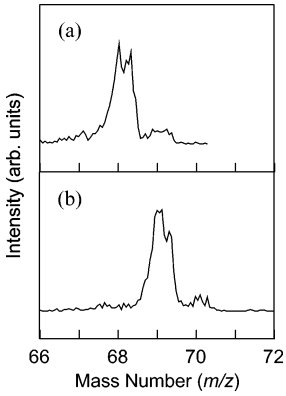

Figure 2. Mass spectra obtained by using the first and the second mass filters in a tandem arrangement. Panels a and b show the mass spectra obtained when the first mass filter is tuned for the 68 amu peak and the 69 amu peak, respectively. The mass spectra demonstrate that CrO^+ and $CrOH^+$ are clearly separated. Note that the peak of 69 amu consists of ∼95% of $^{52}CrOH^+$ and ∼5% of $^{53}CrO^+$ (see the text).

3. Results

3.1. Mass Spectra of Product Ions. Figure 3 shows typical mass spectra of ions produced by a single collision reaction of CrO^+ (panel a) and $CrOH^+$ (panel b) with C_2H_4. Figure 4 shows typical mass spectra of ions produced by a single collision reaction of Cr_2^+ (panel a), Cr_3^+ (panel b), and Cr_2OH^+ (panel c) with C_2H_4. The collision energy was set to be 0.15 eV in the center-of-mass frame. The mass spectra shown in Figures 3 and 4 were measured for obtaining the reaction cross sections so that the mass resolution was reduced to ∼30 for gaining the peak intensity. No reaction product was found to be produced at this collision energy from Cr^+ (consistent with ref 23) and Cr_2O^+. All the product ions given above were proven to be generated by a single collision of C_2H_4 because the intensities of the product ions increase proportionally to the increment of the C_2H_4 pressure. The reactions under multiple collision conditions were examined by increasing the pressure of C_2H_4 gas in the reaction cell from 5×10^{-5} to 7×10^{-4} Torr. Panels c and d of Figure 3 show mass spectra of ions produced from multiple collision of C_2H_4 on CrO^+ (panel c) and on $CrOH^+$ (panel d), respectively. The parent ions, CrO^+ and $CrOH^+$, were found to produce $Cr(C_2H_4)_2^+$ and $CrX(C_2H_4)_{1,2}^+$ (X = O, OH) as a result of the multiple collision of C_2H_4. The mass spectra also revealed that no such reactions occur on Cr_n^+, Cr_nO^+, and Cr_nOH^+ ($n \geq 2$) even by the multiple collision of C_2H_4. Relative ion intensities of the product ions with respect to the total ion intensity including the unreacted parent ion were obtained for

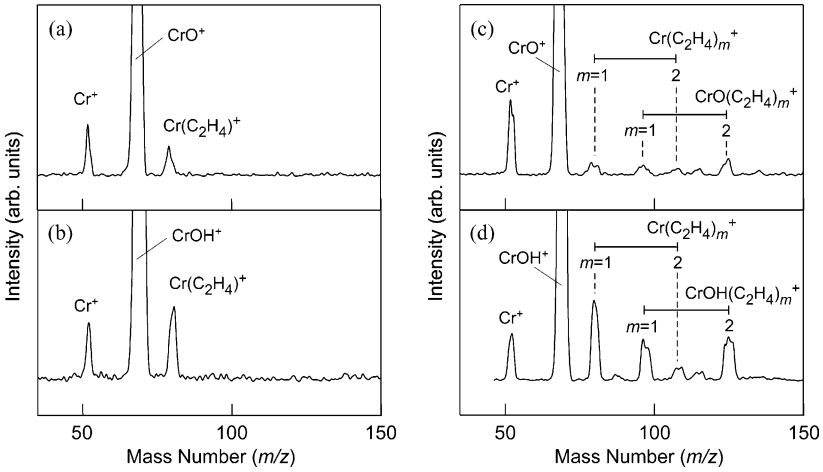

Figure 3. Panels a and b show the mass spectra of ions produced by the collision of CrO^+ and $CrOH^+$ with C_2H_4, respectively, at the collision energy of 0.15 eV under single collision conditions. Panels c and d show the mass spectra for CrO^+ and $CrOH^+$, respectively, under multiple collision conditions. The peak assignments are illustrated in the spectra.

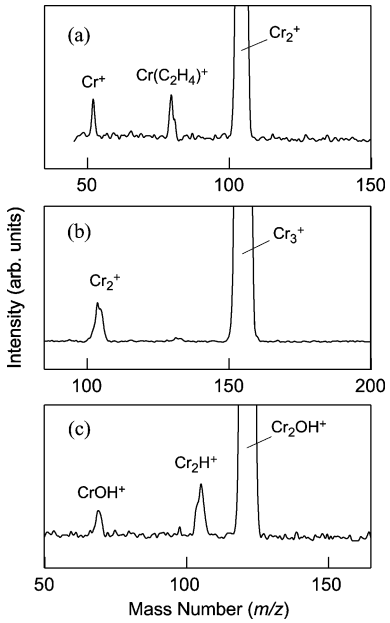

Figure 4. Panels a−c show the mass spectra of ions produced by the collision of Cr_2^+, Cr_3^+, and Cr_2OH^+ with C_2H_4 at the collision energy of 0.15 eV under single collision conditions. The peak assignments are illustrated in the spectra.

the reactions of CrO^+ and $CrOH^+$ with C_2H_4 at the C_2H_4 pressure of 7×10^{-4} Torr and are listed in Table 1. Note that no product ion was observed from Cr^+ even when the pressure was increased to 9×10^{-4} Torr.

3.2. Measurements of Reaction Cross Sections. A total reaction cross section (σ_r) for the production of all the reaction products by a single collision is given as

$$\sigma_r = \frac{k_B T}{Pl} \ln \frac{I_r + \sum I_p}{I_r} \quad (1)$$

where I_r and $\sum I_p$ represent the intensity of an intact parent ion passing through the collision region and the sum of the intensities of the product ions, respectively, P and T are the pressure and the temperature of a sample gas, respectively, l is the effective path length of the collision region, and k_B is the Boltzmann constant. The effective path length, l, has been determined to be 120 ± 3 mm in our previous study[20] by measuring the ion intensities for the reaction

$$Ar^+ + H_2 \rightarrow ArH^+ + H \quad (2)$$

whose absolute cross section is given.[24] A partial cross section, σ_p, for the formation of a given product ion is expressed as

$$\sigma_p = \sigma_r \frac{I_p}{\sum I_p} \quad (3)$$

where $I_p/\sum I_p$ represents the branching fraction for a product ion of interest. The uncertainties in the absolute reaction cross sections consist of (1) systematic errors arising from the uncertainties in the ion collection efficiency and in determining the pressure, P, and the effective path length, l, and (2) statistical errors arising from the fluctuation of the ion intensities. The systematic and the statistical errors were typically 30% and 20%, respectively. The cross sections shown in Figures 5−7 have error bars associated with the statistical errors, because the systematic errors have little effect in arguing the tendency of the cross sections to change depending on the size and the collision energy.

TABLE 1: Relative Intensities of the Product Ions with Respect to the Total Ion Intensity Including the Unreacted Parent Ion Obtained for the Reactions of CrO^+ and $CrOH^+$ with C_2H_4 at the C_2H_4 Pressure of 7×10^{-4} Torr, Where X Represents O or OH

	product				
parent	Cr^+	$Cr(C_2H_4)^+$	$Cr(C_2H_4)_2^+$	$CrX(C_2H_4)^+$	$CrX(C_2H_4)_2^+$
CrO^+	0.060	0.015	0.008	0.011	0.016
$CrOH^+$	0.026	0.029	0.004	0.025	0.048

The mass resolution was not high enough to distinguish parent and product ions from their isotopes in the entire size range studied except for the sizes of 1 and 2. In this experiment, therefore, the cross sections for the parent ions of Cr_nO^+ and Cr_nOH^+ were separately measured only for $n = 1$, 2. Let us consider the reaction of CrO^+ with C_2H_4. The mass peak associated with the parent ion, $^{52}CrO^+$, is well resolved from the other isotopic analogues in the mass spectrum. It is also true for the product ions, $^{52}Cr^+$, $^{52}Cr(C_2H_4)^+$, and $^{52}CrO(C_2H_4)^+$. By taking advantage of these isotopic species, the cross sections for the reaction between CrO^+ and C_2H_4 were obtained. In the

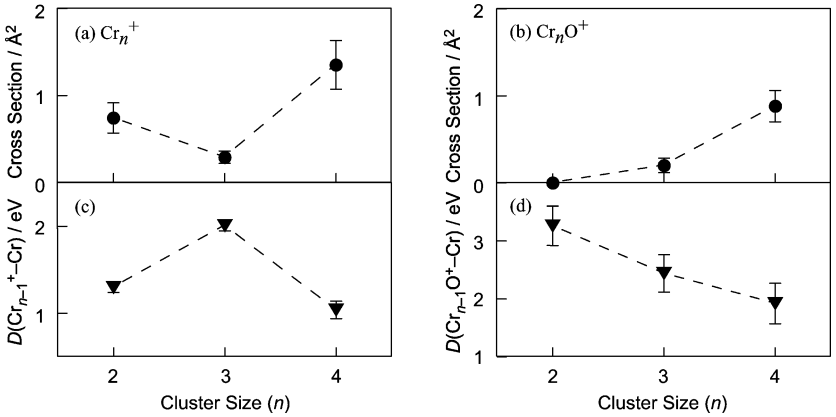

Figure 5. The cross sections for the Cr-pickup reaction involving Cr_n^+ (panel a) and Cr_nO^+ (panel b) at the collision energy of 0.15 eV are plotted against the cluster size, *n*. The error bars give one standard deviation of the statistical errors in the cross sections. The dissociation energies of the Cr_{n-1}^+−Cr (panel c) and the $Cr_{n-1}O^+$−Cr (panel d) bonds taken from refs 30 and 31, respectively, are also plotted against the cluster size, *n*.

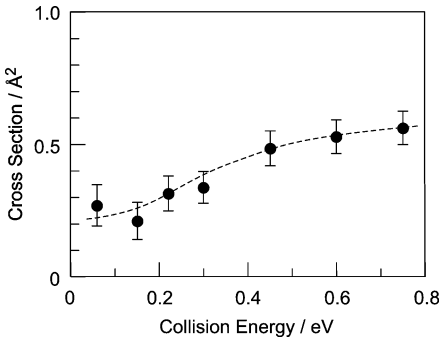

Figure 6. The cross sections for the Cr-pickup reaction involving Cr_3^+ are shown as a function of the collision energy. The error bars give one standard deviation of the statistical errors in the cross sections. The dashed line is an eye-guide.

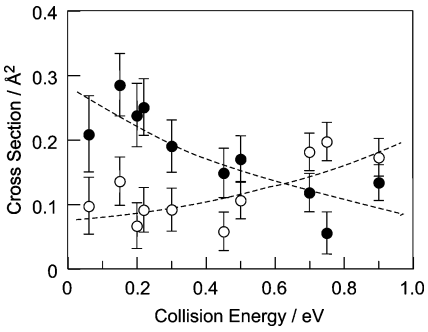

Figure 7. The cross sections for the $Cr_2OH^+ + C_2H_4$ reaction are plotted as a function of the collision energy. The solid and open circles exhibit the cross sections for the Cr-pickup and the C_2H_4 oxidation reactions, respectively. The error bars give one standard deviation of the statistical errors in the cross sections. The dashed lines are eye-guides.

reaction of $CrOH^+$ with C_2H_4, $^{52}CrOH^+$ was chosen as the parent ion having the mass of 69 amu. As $^{53}CrO^+$ contributes to the 69 amu peak by about 5%, the intensity of the 69 amu peak was reduced by 5% as the intensity of the parent ion. The product ion except for $^{52}CrOH(C_2H_4)^+$ was well resolved on the mass spectrum of the product ions. The 97 amu peak associated with $^{52}CrOH(C_2H_4)^+$ coincides with that associated with $^{53}CrO(C_2H_4)^+$. The contribution of $^{53}CrO(C_2H_4)^+$ was estimated from the intensity of $^{52}CrO(C_2H_4)^+$ produced from the parent ion, $^{52}CrO^+$. In the reactions involving Cr_2O^+ and Cr_2OH^+, the intensities of the parent and the product ions were obtained similarly. In the reactions of larger cluster ions, the mass resolution was not high enough to separate well the parent ions Cr_nO^+ from Cr_nOH^+; 10% of Cr_nOH^+ was found to be mixed in Cr_nO^+.

3.3. Dependence of Reaction Cross Sections on Size and Collision Energy. Panels a and b of Figure 5 show the total cross sections for Cr_n^+ and Cr_nO^+ plotted against the cluster size, *n*, at the collision energy of 0.15 eV. Figure 6 shows the total cross sections for the Cr_3^+ collision as a function of the collision energy. The cross section increases slightly with the collision energy; other parent ions, Cr_n^+ and Cr_nO^+, exhibit almost the same collision-energy dependences. Figure 7 shows the collision-energy dependence of the cross sections for the production of $CrOH^+$ (solid circles) and Cr_2H^+ (open circles). As the collision energy increases, the cross section of the $CrOH^+$ production decreases monotonically, whereas that of the Cr_2H^+ production increases.

4. Discussion

4.1. Reaction Processes by Single Collision. *Reactions on CrO^+ and $CrOH^+$.* The reactions of CrO^+ and $CrOH^+$ under the single collision conditions are expressed as

$$CrX^+ + C_2H_4 \rightarrow Cr^+ + C_2H_4X \qquad (C_2H_4 \text{ oxidation}) \quad (4)$$

$$CrX^+ + C_2H_4 \rightarrow CrC_2H_4^+ + X \qquad (C_2H_4 \text{ chemisorption}) \quad (5)$$

where X represents O or OH. In this measurement, any neutral products cannot be detected so that the energetics was applied to determine the counter neutral products. The counter neutral product of Cr^+ is determined to be C_2H_4X on the basis of the energetics that only reaction 4 is exothermic; the dissociation energy of the Cr^+−O bond is 3.72 ± 0.12 eV,[25] the formation energy for the C_2H_4−O bond to form CH_3CHO is 4.85 eV,[26] and the collision energy is 0.15 eV. The energetics denies the progress of such a reaction as

$$CrX^+ + C_2H_4 \rightarrow Cr^+ + C_2H_4 + X \qquad (6)$$

A similar energetics is applicable to the $CrOH^+$ reaction. Kang and Beauchamp have studied a collisional reaction between CrO^+ and C_2H_4 at collision energies of >0.5 eV[27] and reached the conclusion that the neutral counterpart of Cr^+ is CH_3CHO

(acetaldehyde) formed via a reaction intermediate, metallacycle species.

On the other hand, the C_2H_4 chemisorption proceeds conceivably through an intermediate, $[CrX(C_2H_4)^+]^\dagger$, as

$$CrX^+ + C_2H_4 \rightarrow [CrX(C_2H_4)^+]^\dagger \quad (7)$$

$$[CrX(C_2H_4)^+]^\dagger \rightarrow CrC_2H_4^+ + X \quad (8)$$

The neutral counter part of the ionic product is determined unambiguously as X (O or OH). The intermediate, $[CrX(C_2H_4)^+]^\dagger$, has an internal energy which is determined from the initial vibrational energy of the parent ion, the collision energy, and the chemisorption energy of C_2H_4. The chemisorption energies of C_2H_4 on CrO^+ and $CrOH^+$ were obtained from our preliminary density functional theory (DFT) calculation[28] as 3.68 and 2.88 eV, respectively, while the bond energies of Cr^+-O and Cr^+-OH are taken from the reported values of 3.72 ± 0.12 eV[25] and 3.17 ± 0.22 eV,[29] respectively. It is concluded that only the above process (see eqs 7 and 8) is energetically permitted by assuming that the dissociation energy of Cr^+-X does not change with and without C_2H_4.

An ion, $CrX(C_2H_4)^+$, is not produced under the single collision conditions (see section 3.1), because the energy of the reaction intermediate, $[CrX^+(C_2H_4)]^\dagger$, is too large to be maintained in its internal modes over several tens of microseconds and is liberated by releasing X (see eq 8) or C_2H_4.

Reactions on Cr_n^+ and Cr_nO^+ ($n \geq 2$). In a single collision of a cluster ion with C_2H_4, the following chromium pickup (Cr-pickup) reaction proceeds:

$$Cr_n^+ + C_2H_4 \rightarrow Cr_{n-1}^+ + CrC_2H_4 \quad (n = 2-4) \quad (9)$$

$$Cr_n^+ + C_2H_4 \rightarrow Cr_{n-1} + CrC_2H_4^+ \quad (n = 2) \quad (10)$$

$$Cr_nO^+ + C_2H_4 \rightarrow Cr_{n-1}O^+ + CrC_2H_4 \quad (n = 3, 4) \quad (11)$$

Note that a positive charge is located either in Cr_{n-1} or CrC_2H_4 for $n = 2$ only. Therefore the counter neutral product of Cr_{n-1}^+ and $Cr_{n-1}O^+$ must be CrC_2H_4 because the positive ion of the counter neutral product is actually detected in the reaction involving the chromium dimer ion as described above. In addition, collision-induced dissociation such as

$$Cr_n^+ + C_2H_4 \rightarrow Cr_{n-1}^+ + Cr + C_2H_4 \quad (12)$$

$$Cr_nO^+ + C_2H_4 \rightarrow Cr_{n-1}O^+ + Cr + C_2H_4 \quad (13)$$

is unlikely to proceed because the bond dissociation energies of Cr_{n-1}^+-Cr[30] and $Cr_{n-1}O^+-Cr$[31] in the size range of $n = 2-4$ are larger than 1 eV, which is larger than the collision energy studied.

Figure 8 shows a schematic reaction potential for explaining a single collision reaction on Cr_n^+. Suppose that an incoming C_2H_4 molecule is weakly captured by the positive charge of a target ion (Cr_n^+). The capture cross section is given by the Langevin cross section,[32] σ_L, expressed as

$$\sigma_L = \pi\left(\frac{2\alpha}{E_{col}}\right)^{1/2} \quad (14)$$

where α is the polarizability of C_2H_4 (4.25 Å^3),[26] and E_{col} is the collision energy in the center-of-mass frame. The Langevin cross section is calculated to be 105 Å^2 at the collision energy of 0.15 eV and gives the upper limit of the cross section for the

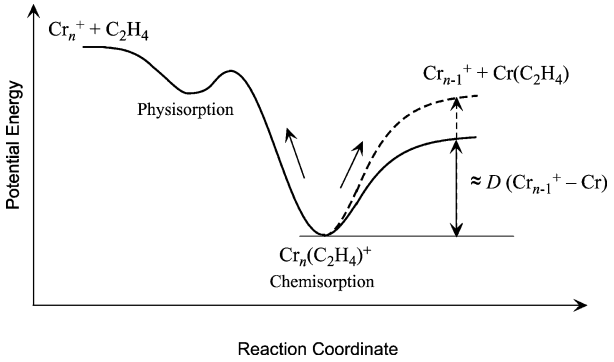

Figure 8. A schematic potential energy curve along the reaction coordinate for the Cr-pickup reaction between Cr_n^+ and C_2H_4. The energy minimum corresponds to the transient ionic species formed by the chemisorption of C_2H_4 on Cr_n^+.

physisorption which preludes the chemisorption. As the reaction cross sections are much smaller than the Langevin cross section, an ionic species ($Cr_n(C_2H_4)^+$) formed temporarily by the chemisorption on Cr_n^+ returns to the original ion (Cr_n^+) by desorbing the C_2H_4 molecule or changes into Cr_{n-1}^+ by releasing CrC_2H_4. A small fraction of the transient ionic species undergoes a Cr-pickup by C_2H_4 (formation of Cr_{n-1}^+) through a rupture of the $Cr_{n-1}^+-CrC_2H_4$ bond. As shown in Figure 5, the cross section for the Cr-pickup exhibits anticorrelation with the dissociation energy of the Cr_{n-1}^+-Cr bond.[30] The anticorrelation implies that (1) the rupture of the $Cr_{n-1}^+-CrC_2H_4$ bond is the rate-determining step and (2) the barrier height toward the Cr-pickup is comparable to the energy of the Cr_{n-1}^+-Cr bond. Note that the chemisorption energy of C_2H_4 on Cr_n^+ is assumed to be practically independent of the cluster size, because the chemisorbed C_2H_4 interacts with two Cr atoms at most. This conclusion does not change significantly even if the parent ion is changed from Cr_n^+ to Cr_nO^+.

Reactions on Cr_2OH^+. In a single collision of Cr_2OH^+ with C_2H_4, $CrOH^+$ and Cr_2H^+ were found to be produced with the neutral counter products of CrC_2H_4 and CH_3CHO, respectively. The former neutral product is most conceivable because it is commonly produced in the other reactions observed, and the latter neutral one is energetically most likely. The reactions are given as

$$Cr_2OH^+ + C_2H_4 \rightarrow CrOH^+ + CrC_2H_4 \quad \text{(Cr-pickup)} \quad (15)$$

$$Cr_2OH^+ + C_2H_4 \rightarrow Cr_2H^+ + CH_3CHO \quad (C_2H_4 \text{ oxidation}) \quad (16)$$

The energetics described below rules out the reactions

$$Cr_2OH^+ + C_2H_4 \rightarrow CrOH^+ + Cr + C_2H_4 \quad (17)$$

$$Cr_2OH^+ + C_2H_4 \rightarrow Cr_2H^+ + O + C_2H_4 \quad (18)$$

Both reactions 15 and 16 are supposed to proceed via a transient ionic species, $Cr_2OH(C_2H_4)^+$, in which C_2H_4 is chemisorbed. Figure 7 shows the dependence of the cross sections for these two reactions (Cr-pickup and C_2H_4 oxidation) on the collision energy. The Cr-pickup is exothermic because its cross section decreases with the collision energy, while the C_2H_4 oxidation is either endothermic or has an energy barrier on its reaction potential. To examine whether the barrier height in the C_2H_4 oxidation is present or not, the energetics is

considered by using the heat of formation of CH_3CHO from C_2H_4 and O (4.85 eV)[26] and the energy difference between Cr_2OH^+ and Cr_2H^+ ($D(Cr_2^+-OH) + D(O-H) - D(Cr_2^+-H)$). The dissociation energy, $D(Cr_2^+-OH)$, is approximated by $D(Cr^+-OH)$ (=3.17 eV),[29] $D(Cr_2^+-H)$ is approximated by $D(Cr_2^+-D)$ (=2.86 eV),[33] and $D(O-H)$ (=4.44 eV)[26] is taken from the literature. It turns out that the C_2H_4 oxidation is exothermic by 0.10 eV. Therefore, it is concluded that the C_2H_4 oxidation has an energy barrier on the reaction potential.

4.2. Reaction Processes by Multiple Collision. *Reactions on CrO^+ and $CrOH^+$.* At a C_2H_4 pressure higher than 3×10^{-4} Torr, a product ion, $Cr(C_2H_4)_2^+$, starts to be observed via the following processes:

$$CrX^+ + C_2H_4 \rightarrow [CrX(C_2H_4)^+]^\dagger \rightarrow Cr(C_2H_4)^+ + X \quad (19)$$

$$Cr(C_2H_4)^+ + C_2H_4 \rightarrow [Cr(C_2H_4)_2^+]^\dagger \quad (20)$$

$$[Cr(C_2H_4)_2^+]^\dagger + C_2H_4 \rightarrow Cr(C_2H_4)_2^+ + C_2H_4 \quad (21)$$

The product ion, $Cr(C_2H_4)_2^+$, is produced from CrX^+ by a triple collision of C_2H_4 because the intensity of $Cr(C_2H_4)_2^+$ increases proportionally to the cube of a C_2H_4 pressure increment. It is likely that two C_2H_4 molecules are adsorbed on CrX^+ into $[Cr(C_2H_4)_2^+]^\dagger$ having a large amount of energy in its internal modes, and the other one C_2H_4 molecule is used for the de-excitation of $[Cr(C_2H_4)_2^+]^\dagger$. In addition, $CrX(C_2H_4)_m^+$ ($m = 1$, 2) is produced by the multiple collision of C_2H_4, that is,

$$CrX^+ + C_2H_4 \rightarrow [CrX(C_2H_4)^+]^\dagger \quad (22)$$

$$[CrX(C_2H_4)^+]^\dagger + C_2H_4 \rightarrow CrX(C_2H_4)^+ + C_2H_4 \quad (23)$$

$$[CrX(C_2H_4)^+]^\dagger + C_2H_4 \rightarrow [CrX(C_2H_4)_2^+]^\dagger \quad (24)$$

$$[CrX(C_2H_4)_2^+]^\dagger + C_2H_4 \rightarrow CrX(C_2H_4)_2^+ + C_2H_4 \quad (25)$$

The ion intensity versus C_2H_4 pressure relationship indicates that about three and four C_2H_4 molecules are involved in the formation of the product ions $CrX(C_2H_4)^+$ and $CrX(C_2H_4)_2^+$, respectively. It implies that double nonreactive collision is required in the de-excitation processes of the intermediates (eqs 23 and 25) on average. A preliminary calculation based on a B3LYP hybrid density functional method reveals that seven kinds of isomers of $CrOH(C_2H_4)_2^+$ are present; a butene complex (the most stable), an ethylene complex (the second most stable), a π-allyl complex, an ethylene and ethylidene complex, a butylidene complex, a metallacycle complex, and a hydrogen and butenyl complex. Therefore, part of the $CrOH(C_2H_4)_2^+$ detected should be in the form of the butene complex because the butene complex is energetically the most stable. In other words, $(C_2H_4)_2$ in the product ion, $CrOH(C_2H_4)_2^+$, is dimerized into butene. It is reasonable to consider that $(C_2H_4)_2$ in the product ion, $CrO(C_2H_4)_2^+$, is also dimerized into butene, although no calculation has been made at the present stage.

The relative ion intensities of the product ions at the pressure of 7×10^{-4} Torr are relatively small (see Table 1) because the pressure of ethylene gas in the reaction cell is not sufficiently high. The pressure dependence of the intensities of $Cr(C_2H_4)_2^+$ and $CrX(C_2H_4)_2^+$ in the pressure range of $2-9 \times 10^{-4}$ Torr reveals that three or four collisions are necessary to generate $Cr(C_2H_4)_2^+$ and $CrX(C_2H_4)_2^+$ as described above. Actually, both of the parent cluster ions, CrO^+ and $CrOH^+$, collide with ethylene molecules three times or less on average in the reaction cell; the collision frequency is not sufficient to generate and stabilize $Cr(C_2H_4)_2^+$ and $CrX(C_2H_4)_2^+$. In any case, it is obvious from Table 1 that the parent ion, $CrOH^+$, is much more capable of adsorbing ethylene molecules than CrO^+. Higher reactivity of $CrOH^+$ is explained as follows: (1) The number of internal modes of $CrOH^+$ is larger than that of CrO^+; the transient ionic species, $[CrOH(C_2H_4)^+]^\dagger$, has a larger number of internal modes than $[CrO(C_2H_4)^+]^\dagger$, so that the adsorption energy of C_2H_4 is more readily redistributed into the internal modes. (2) The density of d-electrons on the Cr site in $CrOH^+$ is larger than that of CrO^+ because the O atom acts as a strong electron-withdrawing group; in the framework of the Dewar−Chatt−Duncanson donor−acceptor model,[34,35] the olefin complex on the metal is stabilized by the electron back-donation from the metal 3d orbital to the olefin π^* orbital.

Active Center for Ethylene Polymerization. As described above, the present results provide important information on the active center of the Phillips catalyst, because the catalyst is composed of chromium supported on a silica powder and hence the polymerization on the catalyst can be compared with the reactions occurring on Cr_n^+, Cr_nO^+, and Cr_nOH^+ clusters. The fundamental feature of the gas-phase reaction is summarized as follows: (1) Ethylene molecules are chemisorbed on CrO^+ and $CrOH^+$ and are polymerized into butene as shown by a DFT calculation, and (2) an ethylene molecule is simply chemisorbed on Cr_n^+, Cr_nO^+, and Cr_nOH^+ ($n \geq 2$) but released as CrC_2H_4. These findings indicate that the active center of the Phillips catalyst should be an atomic chromium bonded to O or OH of the silica substrate. On the other hand, intensive investigations of the Phillips catalyst have shown that the active center for ethylene polymerization on the catalyst is either an atomic chromium site[5,15] or a diatomic chromium site,[16,17] although this issue has not yet been settled.

5. Conclusion

In the present study, we investigated the reactions of ethylene on chromium cluster ions and their monoxides and hydroxides in the gas phase and found that only chromium monoxide and hydroxide ions are able to catalyze ethylene dimerization; its catalytic activity is diminished by adding one more chromium atom to it. These results indicate that in the Phillips catalyst an atomic chromium bonded to O and OH of its substrate is the active center for ethylene polymerization; the Phillips catalyst is made of chromium which is supported on silica. This methodology is applicable to identify the most efficient reaction site on a heterogeneous catalyst.

Acknowledgment. The authors thank Mr. Haruhiko Kadowaki for his assistance in the experiment. This work was supported by the Special Cluster Research Project of Genesis Research Institute, Inc.

References and Notes

(1) Riley, S. J. In *Clusters of Atoms and Molecules II*; Haberland, H., Ed.; Springer-Verlag: Berlin, 1994; p 221. Anderson, S. L. In *Clusters of Atoms and Molecules II*; Haberland, H., Ed.; Springer-Verlag: Berlin, 1994; p 241.

(2) Knickelbein, M. B. *Annu. Rev. Phys. Chem.* **1999**, *50*, 79.

(3) Bond, G. C. In *The Physical Basis for Heterogeneous Catalysis*; Drauglis, E.; Jaffee, R. I., Eds.; Plenum Press: New York, 1975; p 53.

(4) Hogan, J. P.; Banks, R. L. Belg. Patent 530617, 1955.

(5) Hogan. J. P. In *Applied Industrial Catalysis*; Leach, B. E., Ed.; Academic Press: New York, 1983; Vol. 1, p 149.

(6) McDaniel, M. P. *Adv. Catal.* **1985**, *33*, 47.

(7) Weckhuysen, B. M.; Schoonheydt, R. A. *Catal. Today* **1999**, *51*, 215.

(8) Myers, D. L.; Lunsford, J. H. *J. Catal.* **1985**, *92*, 260.

(9) Wang, S.; Tait, P. J. T.; Marsden, C. E. *J. Mol. Catal.* **1991**, *65*, 237.
(10) McDaniel, M. P.; Martin, S. J. *J. Phys. Chem.* **1991**, *95*, 3289.
(11) Hogan, J. P.; Norwood, D. D.; Ayres, C. A. *J. Appl. Polym. Sci.*: *Appl. Polym. Symp.* **1981**, *36*, 49.
(12) McDaniel, M. P. *Ind. Eng. Chem. Res.* **1988**, *27*, 1559.
(13) Marsden, C. E. *Plast. Rubber Compos. Process. Appl.* **1994**, *21*, 193.
(14) Wechhuysen, B. M.; Wachs, I. E.; Schoonheydt, R. A. *Chem. Rev.* **1996**, *96*, 3327.
(15) Krauss, H. L.; Hums, E. *Z. Naturforsch., B*: *Anorg. Chem., Org. Chem.* **1979**, *34b*, 1628.
(16) Rebenstorf, B.; Larsson, R. *J. Mol. Catal.* **1981**, *11*, 247.
(17) Rebenstorf, B. *J. Mol. Catal.* **1989**, *56*, 170.
(18) Brucat, P. J.; Pettiette, C. L.; Yang, S.; Zheng, L.-S., Craycraft, M. J.; Smally, R. E. *J. Chem. Phys.* **1986**, *85*, 4747.
(19) Berg, C.; Beyer, M.; Achatz, U.; Joos, S.; Niedner-Schatteburg, G.; Bondybey, V. E. *J. Chem. Phys.* **1998**, *108*, 5398.
(20) Hirokawa, J.; Ichihashi, M.; Nonose, S.; Tahara, T.; Nagata, T.; Kondow, T. *J Chem. Phys.* **1994**, *101*, 6625.
(21) Ichihashi, M.; Hanmura, T.; Yadav, R. T.; Kondow, T. *J. Phys. Chem. A* **2000**, *104*, 11885.
(22) Ingólfsson, O.; Takeo, H.; Nonose, S. *J. Chem. Phys.* **1999**, *110*, 4382.
(23) Georgiadis, R.; Armentrout, P. B. *Int. J. Mass Spectrom. Ion Processes* **1989**, *89*, 227.
(24) Ervin, K. M.; Armentrout, P. B. *J. Chem. Phys.* **1985**, *83*, 166.
(25) Fisher, E. R.; Elkind, J. L.; Clemmer, D. E.; Georgiadis, R.; Loh, S. K.; Aristov, N.; Sunderlin, L. S.; Armentrout, P. B. *J. Chem. Phys.* **1990**, *93*, 2676.
(26) Lide, D. R. *CRC Handbook of Chemistry and Physics*, 78th ed.; CRC Press: Boca Raton, FL, 1997.
(27) Kang, H.; Beauchamp, J. L. *J. Am. Chem. Soc.* **1986**, *108*, 5663.
(28) Hanmura, T.; Ichihashi, M.; Monoi, T.; Matsuura, K.; Kondow, T. In preparation.
(29) Kang, H.; Beauchamp, J. L. *J. Am. Chem. Soc.* **1986**, *108*, 7502.
(30) Su, C.-X.; Armentrout, P. B. *J. Chem Phys.* **1993**, *99*, 6506.
(31) Griffin, J. B.; Armentrout, P. B. *J. Chem. Phys.* **1998**, *108*, 8075.
(32) Levine, R. D.; Bernstein, R. B. *Molecular Reaction Dynamics*; Oxford University Press: Oxford, 1974.
(33) Conceição, J.; Liyanage, R.; Armentrout, P. B. *Chem. Phys.* **2000**, *262*, 115.
(34) Dewar, M. J. S. *Bull. Soc. Chim. Fr.* **1951**, *18*, C71.
(35) Chatt, J.; Duncanson, L. A. *J. Chem. Soc.* **1953**, 2939.